A Method for Simultaneous Optimization of Power Management Schedule and Flight Trajectory for Hybrid Electric Aircrafts

HyunKi Lee [†‡]
hlee389@gatech.edu

The aviation industry relies on a diverse set of objectives to operate at optimal efficiency and profitability. Two of these objectives are reducing emission and flight trajectory generation during flight. To address the first goal, there is an increasing interest in aircraft hybridization in the industry due to its potential to meet future performance and environmental goals. The primary challenge of creating a hybrid aircraft is to find the balance between two energy sources, electric and gas turbine power, to generate the required thrust. Optimizing the power split trajectory for a fixed mission can reduce fuel burn. Fulfilling the second goal of optimizing the mission trajectory is another way of minimizing fuel burn. In fact, the expected reduction is the greatest when you simultaneously optimize the mission trajectory and the power split trajectory. This paper proposes a single approach that attempts to fulfill the two aforementioned objectives at once and during flight. Differential dynamic programming (DDP) is proposed to generate flight trajectory while considering the optimal gas and electric power split to minimize fuel burn. A notable strength of the DDP lies in its speed. Hence, it could assist pilots during flight. DDP is applied to a 9 passenger jet aircraft airframe with a series hybrid architecture turboprop engine. The series hybrid architecture is chosen based on the potential for emission reduction observed in the automobile industry using this architecture. The performance of the optimized aircraft is compared to the performance of the non hybrid aircraft for a nominal turboprop aircraft mission to observe the potential of this method. The challenge with this formulation is the increase in problem dimension. Although electric power has a lower life cycle emission than gas turbine, the increasing weight from the electric components results in higher fuel consumption. Trade study is performed on the algorithm for hybrid configuration to analyze the aircraft performance in various hyperparameter settings. Finally, a baseline framework is proposed for this methodology.

I. Motivation

THE air traffic demand has been on the rise at a steady pace from 4,500 Billion passenger kilometers to 8,200 Billion passenger kilemeters between years 2009 and 2018, as shown in Fig.1[1]. With the increasing demand for air traffic, the pressure on emission reduction from aviation industry increases. NASA has set an aggressive goal for next generation aircrafts to reduce emission up to 75 percent by the third generation aircraft as shown in Table1[2].

Table 1 NASA near (N+1) to far (N+3) term emission goals

Technology Benefits	N+1	N+2	N+3
Noise	-32dB	-42dB	-71dB
LTO NOx Emissions	-60%	-75%	<-75%
Aircraft Fuel Burn	-33%	-50%	<-70%
Field Length	-33%	-50%	–

[†]Graduate Research Assistant, Aerospace System Design Laboratory, School of Aerospace Engineering, Georgia Institute of Technology

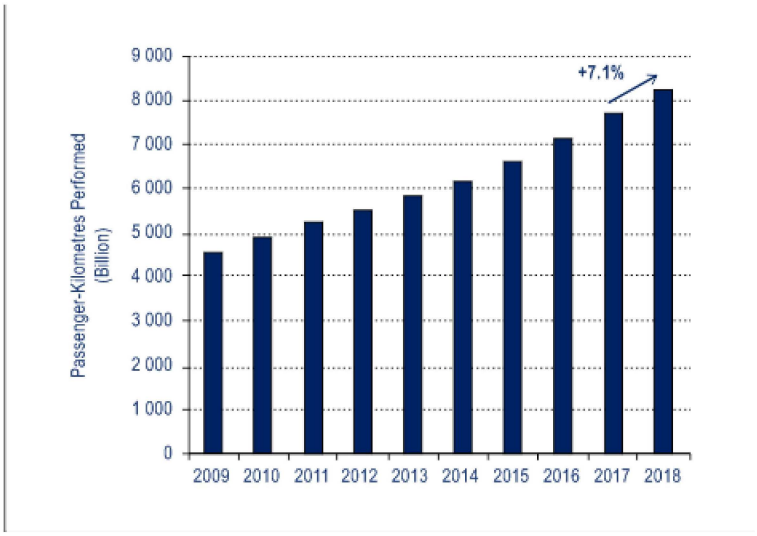

Fig. 1 Passenger Kilometers Performed For Total Scheduled Traffic 2009-2018

Conventional gas turbine architecture fails to satisfy this goal so alternate concept aircrafts are considered including the hybrid electric engine architecture aircrafts. This type of aircraft can replace or combine mechanical power distribution system with electric power distribution system. It allows for an innovatinve configurations such as blended wing and fully turboelectric systems that has the potential of reducing the emission by 50 to 70 percent[2].

The potential benefit of utilizing hybrid architecture comes with a power management challenge. The conventional gas turbine aircraft utilizes single energy source and the engine power to satisfy a required thrust is simply matched by the gas turbine as shown in Eq. 1a. With the hybrid architecture, required thrust is obtained by combining the electric and gas turbine power generated by the battery and the fuel as shown in Eq. 1b.

$$\mathbf{T}_{required} = \mathbf{T}(\mathbf{P}_{GasTurbine}) \tag{1a}$$

$$\mathbf{T}_{required} = \mathbf{T}(\mathbf{P}_{Batt}, \mathbf{P}_{GasTurbine}) \tag{1b}$$

Utilizing only the electric power would reduce the fuel use but increase the total aircraft weight during flight since the aircraft needs to carry a heavier battery. Increased aircraft weight results in larger propulsion system and life cycle emission. In fact with the current technology, the specific energy of the battery is much lower than fuel and typical missions can not be performed while utilizing only the battery power. Impact of weight on the aircraft efficiency can be observed from the conventional aircraft data[3]. On the contrary, utilizing only the mechanical power would result in increased emission during flight but the total aircraft weight reduces, hence a potentially more efficient flight. So an optimization method that balance the power split of these two sources is necessary to minimizing fuel burn and emission.

Optimizing mission trajectory is another way of minimizing fuel burn. Due to the significant impact the flight conditions have on the engine performance, fuel burn reduction is expected by generating the optimal route to fulfill the mission. NASA has also set a goal of optimizing the mission trajectory on the fly to assist pilots decision making[4]. Multiple algorithms exist to not only generate the optimized trajectory but also a dynamic trajectory that is robust to disturbance [5] or a trajectory designed to fly around physical constraints such as buildings and projectiles[6]. At the core of these algorithms are the objective functions, a single metric defined by the current state of the aircraft and input commands. Converging the objective function to a minimum will allow the states to reach the target location with the minimum input command. For this paper, the aircraft states can be defined by the position, energy consumption, and electric vs gas turbine power split of the aircraft. By minimizing the objective function, the flight trajectory with optimal power split to minimize fuel burn is determined. A similar attempt was made in the automobile industry with a Toyota Prius II model where the velocity trajectory optimized with different value of α (electric vs mechanical power split)[7]. However, this method does not consider factors that are critical to flight, such as weight of the aircraft at a given time. Also, the significant difference in the dynamics requires to investigate this method for an aircraft separately.

The purpose of this paper is to propose a framework for simultaneous flight trajectory and power management optimization method for the hybrid aircraft. The goal is to minimize fuel burn of a hybrid aircraft over a typical commercial aircraft mission phase. Then compare the optimized trajectory and the fuel use for conventional aircraft vs

hybrid architecture aircraft. Section II will discuss the hybrid electric architectures. Section III will discuss the litierature review of the methods for optimizing power management and trajectory. Section IV will discuss the background of optimization methods, dynamics of the aircraft model, and the method applied in this paper. Section V will discuss the implementation of the proposed methodology. Finally section VI will present the results.

II. Hybrid Electric Architectures

Hybrid electric architectures combine gas turbine and electric motors to generate the total power required for the desired thrust. This concept is proposed to reduce the life cycle emission of an aircraft for a given mission. Two major types of hybrid electric architectures include series hybrid, such as the Zunum Aero, and parallel hybrid, such as the Boeing Sugar Volt. The advantages of a fully electrified propulsion system is reduced emission during mission, reduced atmospheric heat release, reduced noise and increased engine efficiency. However, with current technology, batteries lack specific energy. Hence, hybrid architecture is required to fly an aircraft that is electrified[8].

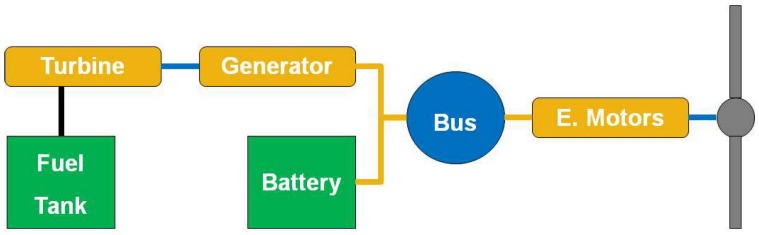

Fig. 2 Series Hybrid Architecture Setup Diagram

Fig.2 displays a series hybrid engine with two energy source. Green boxes indicate energy sources, yellow boxes indicate power generator, blue circle indicates power split component, and the grey geometry indicates a fan. The black line represents a pipe, blue line represents a shaft, and the yellow lines represent electric cords. As shown, series architecture typically have an electric motor turning the fan and an electric power distribution system. The benefit is that engine is decoupled from the transmission, so the engine can always turn at the optimum efficiency. However, there is a penalty of added weight due to the extra generator.

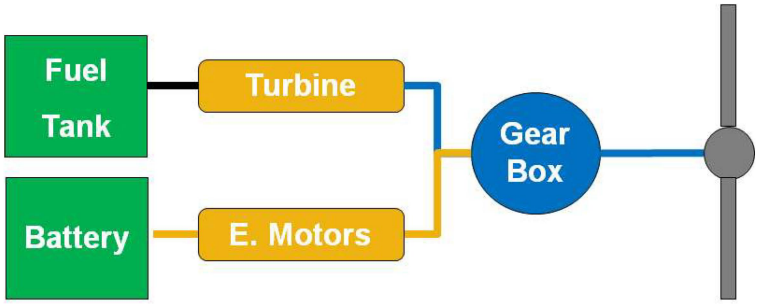

Fig. 3 Parallel Hybrid Architecture Setup Diagram

Fig.3 displays a parallel hybrid engine with two energy sources. The same color coding is applied as Fig.2. The benefit is that both gas turbine and electric motor are connected to the shaft so one system can be used as main power source. However, this increases the control complexity and mechanical coupling of each component where turbine and electric motor are connected to a gearbox, which turns the fan. Both types of propulsion system require a method for optimizing power split (λ) beteween electric motor and gas turbine to minimize the fuel use. For this paper, series hybrid architecture aircraft model is used because of the need to create a baseline for this type of aircraft. There is a lack of knowledge in the series hybrid architecture compared to that of the parallel hybrid even though there is a need for series hybrid architecture, such as Zunum Aero.

III. Literature Review

Power split and trajectory optimization are problems that are frequently studied. The goal for these optimization problems is to find the control vector trajectory, u(t), that would minimize the objective function, $J(u)$

$$J = \phi(x(t_f)) + \int_{t_0}^{t_f} L(x(t), u(t), t)dt \tag{2}$$

subject to

$$\dot{x}(t) = f(x(t), u(t)) \tag{3}$$

where ϕ is the terminal cost and L is the running cost. If L is minimized subjet to a constraint then

$$L(x(t), u(t), t) = l(x(t), u(t), t) + \lambda(f(x(t), u(t), t) - \dot{x}) \tag{4}$$

where $f(x, u, t) = \dot{x}$ is the performance constraint and l is the function to be minimized. The Hamiltonian function is defined as

$$H(x(t), u(t), \lambda(t), t) = l(x(t), u(t), t) + \lambda^T(t) f(x(t), u(t), t) \tag{5}$$

and to minimize the objective function, the Hamiltonian function is minimized to solve for the Hamilton Jacobi Bellman equation (HJB), defined as

$$\frac{\delta H^T}{\delta u} = 0 \tag{6}$$

The HJB equation provides the necessary condition to minimize the objective function. Also, the costate trajectory λ exist for optimal x(t) and u(t) trajectory, under Pontryagin's maximum principle, as long as the following arguments are held, given $0 \leq t \leq T$:

$$\dot{x} = H_\lambda(x(t), u(t), \lambda(t)) \tag{7a}$$

$$-\dot{\lambda} = H_x(x(t), u(t), \lambda(t)) \tag{7b}$$

$$u = \underset{u}{argmin} H(x(t), u(t), \lambda(t)) \tag{7c}$$

Under the specific case where the dynamics is linearized and the objective function is defined as the quadratic functions of x and u, optimal control problem can be analyzed. In this case the optimal control input can be redefined as linear state feedback where the feedback gain (K) is defined by

$$u(t) = -K(t)x(t) \tag{8a}$$

$$K(t) = R^{-1}B^T S(t) \tag{8b}$$

where S(t) is the solution to the Ricatti equation. One type of optimization problem resolves this feedback control vector per time step until the state vector reaches the target[9]. Another type of optimization method, the shooting method, generates full trajectories in different directions until the objective function is minimized. The shooting method is frequently utilized on line due to the reduced computation power and time required. Both optimization methods are utilized to optimize either the flight path or the power split.

A. Power Management Optimization

DOE method is utilized as a way of optimizing power management. During each optimizer run, given number of combinations of λ and other input commands are tried to perform a mission phase of interest. Each input would vary within the typical range observed for existing similar aircraft types. For example λ would vary from 0 (conventional gas turbine) to 1 (fully turbo electric) to compare the performance results based on the power split. The set of inputs that results in minimum fuel burn is chosen. Issue with this method is that the input commands do not vary within each run. Also, there is no guarentee that the combination or min max range of each input command results in a local optimum.

Studies were conducted by Konstantinos [10] and David [11] to minimize fuel burn by finding the optimal power split trajectory λ.

$$J = \dot{w_f}(P_e) + \lambda \dot{SOC}(P_e, SOC) \tag{9}$$

Minimizing algorithm such as golden section or optimal control methods are utilized to find the optimal λ trajectory that generates the required power at each time step. Both methods did result in a λ trajectory that used less fuel than

when λ was fixed at a value. However the fuel reduction is minimal (typically $\leq 1\%$). David [11] also mentioned a dynamic programming method for finding λ trajectory to minimize fuel burn. This method discretizes the battery state of charge and time and determine the optimal battery state of charge trajectory to minimize fuel consumption. None of these methods simultaneously consider optimization of the aircraft flight trajectory to reduce fuel consumption.

Trajectory optimization algorithm has been implemented on the engine and generator efficiency path to improve overall efficiency of the aircraf and minimize the fuel use. Carlos et et. [12] introduced a way of finding the optimal efficiency path by defining the cost function with the energy of the generator and the energy lost due to efficiencies.

$$J = h_1(W_{Generator} - W_{ref})^2 + h_2(W_{loss})^2 \tag{10}$$

For this method, dynamics is defined by the torque of the engine, generator, and the resistive torque. Generator and engine efficiency maps, in terms of torque and speed, are utilized to find the optimal efficiency path. The path would simultaneously maximize the efficiency of the generator and the efficiency of the engine while satisfying the required torque from the dynamics. The optimized fuel use is modeled for three different cases that considers low energy requirement with enough time, high energy requirement with enough time and fast energy production. Unfortunately this method also does not address the flight path optimization for reducing fuel burn.

B. Trajectory Optimization

Falck et el. [13] investigated on finding the optimal flight path with thermal constraint in consideration for the NASA X-57 Maxwell aircraft using local optimum method. Unlike a gas turbine where the only source of heat is the turbine itself, electric components generate heat everywhere, even the cords. Heat is an important factor for determining the efficiency of electrical components. The objective function of this method is a function of range and efficiency subject to temperature, altitude, and velocity of the aircraft. This method utilizes 2D equations of motion where only the longitudinal motion is considered for the aircraft dynamics. The trajectory is found using an optimal control approach based on Legendre Gauss Lobatto collocation method. The results showed a varying flight path with and without temperature constraint and concludes that the motor thermal limit is main limiter for achieving the required climb rate. The problem optimize the efficiency of the subsystems but it doesn't directly address the issue of minimizing fuel use.

Gockin [14] analyzed the optimal trajectory path for climb, cruise, and descent separatly. For each flight phase the path is discretized and vehicle performance is calculated at each discretized states. Optimal trajectory is found by finding the path that results in minimal objective function for reaching the next discretized state. The climb segment is discretized by energy height generated on an altitude-Mach number map. The minimum energy to climb is found by maximizing the energy function, defined by the excess power of the aircraft at each state and the average rate of change of energy at each state. This results in a optimal flight path for every time step but that does not guarentee a local optimum solution for the entire trajectory.

To better minimize the hybrid aircraft emission, through reduced fuel consumption, the following needs to be satisfied: the aircraft needs to fly at the optimized power split trajectory, fly in the optimized flight path for a given misssion, and be designed to fly that optimized flight path. The goal of this paper is to investigate a method that can satisfy the first two conditions simultaneously and guarentee a local optimal solution. Not only that, but the trajectory optimization needs to be able to perform on the fly to assist the pilots decision making. Based on the review, a shooting algorithm that utilize dynamic programing on 2D dynamicis of the aircraft can satisfy the goal. So differential dynamic programming (DDP)[15] with linearized dynamics and quadratic approximation of the cost function is used for this study.

IV. Background

A. Optimization Theory

This section describes the basics of DDP and dynamic model of the aircraft [16]. The objective function, denoted by J, is defined by the total cost of taking the trajectory. The total cost is defined by the sum of running cost (l) and final cost (l_f) incurred from the input command u and initial state x_o until the total number of discretized time steps, also known as horizon (N), is reached.

$$J(x_o, u) = \Sigma_{i=0}^{N-1} l(x_i, u) + l_f(x_N) \tag{11}$$

The objective function is observed for the dynamics of the system defined by a generic function f, trajectory state at time step i (x_i), input command at time step i (u_i), and the trajectory state at input i+1 (x_{i+1}). Where the trajectory state

and input are defined by $X = \{x_0, x_1, ..., x_N\}$ and $U = \{u_0, u_1, ..., u_{N-1}\}$.

$$x_{i+1} = f(x_i, u_i) \tag{12}$$

The value function (V) at any given time i is defined by minimizing the objective function in terms of the input commands.

$$V_i(x) = \min_{u_i} J_i(x_i, u_i) = \min_{u} [l(x, u) + V_{i-1}(x, u))] \tag{13}$$

The benefits of differential dynamic programming are as follows:

1) second order convergence [17]
2) reduced computation time [18]
3) various applications the algorithm succeeded in [19] [20] [21]

B. Differential Dynamic Programming

Differential dynamic programming, DDP, utilizes first order estimation of the dynamics

$$x_{i+1} = (I + f_x)x_i + f_u u_i \tag{14}$$

Where f_x is first order change in the dynamics with state and f_u is first order change in the dynamics with input. DDP utilizes quadratic estimation of the objective function. The second order value function is represented as follows:

$$V = \frac{1}{2} x_N^T l_{f\,xx} X_N + \frac{1}{2} \Sigma_{i=0}^{N-1} (x_i^T l_{xx} x_i + u_i^T l_{uu} u_i) \tag{15}$$

The linearized dynamics and quadratic objective function are reiterated by DDP until the objective function converges to a minimum. Each iteration is done in four large steps:

1) forward propagation of the dynamics with u_i
2) backward propagation of the objective function
3) calculation of new input trajectory $u_{i+1} = u_i + \delta u * \gamma$
4) forward propagation of the dynamics with u_{i+1}

Where γ represents the learning rate. Once the initial forward propagation is performed, the l_f of the value function is integrated back to the initial position to find the total cost of the trajectory. Let Q be the discrete time representation of change in objective function per time step. The quadratic expansion of Q is as follows[16]:

$$Q_x = l_x + f_x^T V_x^{i-1} \tag{16a}$$

$$Q_u = l_u + f_u^T V_x^{i-1} \tag{16b}$$

$$Q_{xx} = l_{xx} + f_x^T V_{xx}^{i-1} f_x \tag{16c}$$

$$Q_{ux} = l_{ux} + f_u^T V_{xx}^{i-1} f_x \tag{16d}$$

$$Q_{uu} = l_{uu} + f_u^T V_{xx}^{i-1} f_u \tag{16e}$$

$$\tag{16f}$$

Modification of u_i is done by estimating δu by some perturbation in x.

$$\delta u(\delta x) = \min_{\delta u} Q = l_i + L_i * \delta x \tag{17a}$$

$$l_i = -Q_{uu}^{-1} Q_u \; and \; L_i \tag{17b}$$

$$= -Q_{uu}^{-1} Q_{ux} \tag{17c}$$

where l_i and L_i are local feedback policy. The feedback policy is used to rederive the value function with the follows:

$$V_i = V_{i+1} + \frac{1}{2} l_k^T Q_{uu} l_k \tag{18a}$$

$$V_x = Q_x + L_k^T Q_u + Q_{xu} l_k + L_k^T Q_{uu} l_k \tag{18b}$$

$$V_{xx} = Q_{xx} + Q_{xu} L_k + L_k^T Qux + L_k^T Quu L_k \tag{18c}$$

The V_N, that defines the initial V_{i+1} is manually predefined by $l_f(x_N)$.

C. Aircraft Dynamics

DDP requires the dynamics of the system to be defined. Aircraft dynamics with typical tube and wing configuration has symmetry in the x and z axis in the body reference frame as shown in Fig.4[22]. Hence, independent longitudinal

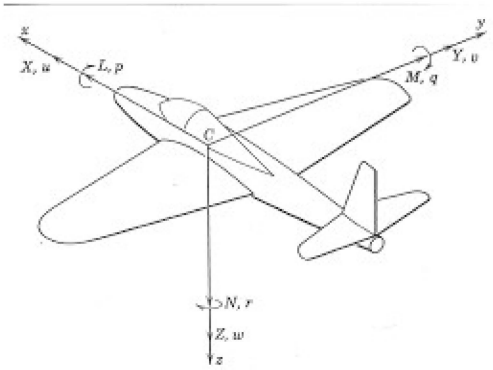

Fig. 4 Notation for body fixed reference frame

and lateral dynamics of the aircraft can be defined based on Etkin and Reid's textbook [23]. Etkin and Reid divides the aircraft dynamics into longitudinal and lateral dynamics. Longitudinal dynamics concerns the linear motion in x and z axis and angular motion in y axis, represented by $[u, \dot{u}, w, \dot{w}, q, \dot{q}]$. Lateral dynamics concerns the linear motion in y axis and angular motions in x and z axis, represented by $[v, \dot{v}, p, \dot{p}, r, \dot{r}]$. Longitudinal and Lateral dynamics can be summarized as equations 19 and 20 with input vector defined by δ. Longitudinal dynamics of a tube and wing aircraft:

$$\begin{pmatrix} u \\ w \\ \dot{w} \\ q \end{pmatrix} = A \begin{pmatrix} x \\ z \\ w \\ \theta \end{pmatrix} + B\delta \tag{19}$$

Lateral dynamics of a tube and wing aircraft:

$$\begin{pmatrix} v \\ p \\ r \end{pmatrix} = A \begin{pmatrix} y \\ \phi \\ \psi \end{pmatrix} + B\delta \tag{20}$$

Since mission analysis typically concern the longitudinal motion of the aircraft and to reduce the scope of the paper, only the longitudinal dynamics is considered. However, lateral dynamics can be included to the dynamics of the algorithm to yield a 6 degree of freedom result for optimal trajectory.

The small disturbance longitudinal dynamics is represented as follows:

$$\frac{d}{dt}u - X_u u + g_0 \cos\Theta_0 \theta - X_w w = X_{\delta_e}\delta_e + X_{\delta_T}\delta_T \tag{21a}$$

$$-Z_u u + \frac{d}{dt}w - Z_{\dot{w}}\frac{d}{dt}w - Z_w w - u_0 q + Z_q q + g_0 \sin\Theta_0 \theta = Z_{\delta_e}\delta_e + Z_{\delta_T}\delta_T \tag{21b}$$

$$-M_u u - M_{\dot{w}}\frac{d}{dt}w + M_w w + \frac{d}{dt}q - M_q q = M_{\delta_e}\delta_e + M_{\delta_T}\delta_T \tag{21c}$$

The longitudinal motion is further simplified by adding following asusmptions:

1) Installed thrust and aerodynamic drag act in the same direction as the velocity
2) Significant forces are thrust (T), lift (L), drag(D), and weight(mg) of the aircraft
3) Significant derivatives are longitudinal derivatives

The reference frame is also changed to earth surface earth fixed reference frame so that the dynamics of the aircraft

would reference the motion observed on earth surface. This would result in the following longitudinal dynamics:

$$m\frac{d}{dt}u = T\cos\theta - D\cos(\gamma) - L\sin(\gamma) \tag{22a}$$

$$m\frac{d}{dt}w = T\sin\theta + L\cos\gamma - D\sin\gamma - mg \tag{22b}$$

$$I_{yy}\dot{q} = M_q q + M_u u + \Delta M_{\delta_e}\delta_e + \Delta M_{\delta_T}\delta_T \tag{22c}$$

where γ is the flight path angle, α is the angle of attack, and θ is defined by $\gamma + \alpha$.

V. Approach

A. Framework

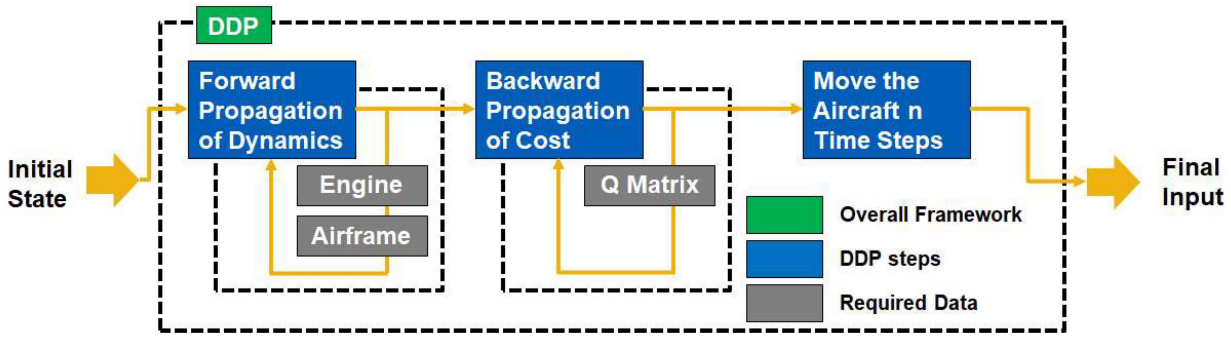

Fig. 5 Proposed methodology framework

Overall framework of the methodology is summarized in Figure 5. The backbone of this methodology is the DDP which generates an optimized flight trajectory that minimizes fuel burn, with power split in consideration. Mainly two sets of external data are required to set up the DDP. First is the airframe geometry data to obtain the drag polar of the aircraft. The airframe model used for this paper is a 9 pax turboprop aircraft with a conventional tube and wing. The Cessna 550 Citation II is an existing nonhybrid architecture aircraft this configuration is comparable to. Zunum Aero is another 9 pax aircraft currently under development with series hybrid architecture engine. Airframe data for Zunum Aero like aircraft is obtained by approximating the geometry and size of each airframe component. Then aircraft drag polar is obtained by flying the airframe data with fixed propulsion settings in FLOPS. FLOPS is NASA's Flight Optimization System used for estimating vehicle empty weight and drag polars for a design mission.

Second data is an engine deck that determines the engine thrust based on the input thrust control, input electric power, and the ambient state. Series hybrid engine deck for a 9pax aircraft is modeled in Numerical Propulsion System Simulation (NPSS). NPSS is designed by NSA and consortium of leading firms within the aerospace industry. NPSS designs the engine based on a user defined model that size for the system weight. This is done by finding the maximum power required for each component of the engine at predefined points in the mission that are expected to push each components of the engine to the limit. Then finding the total weight by multiplying the maximum power of each component by the component specific power. Engine deck generated by NPSS calculates the engine thrust based on Mach number, altitude, power code, and input electric power. In the process it also outputs fuel consumption and corresponding power split used to generate the thrust that match the inputs.

The behavior of an engine is highly nonlinear, which means the interpolation of the engine dynamics may not wholely capture the engine behavior. As shown in Fig.6 [11], linearization may lead to stepwise performance of the engine and a large error for highly nonlinear regions. To resolve this issue surrogate model of the engine deck is made in the JMP statistical software. Surrogate models are generated with 2nd order full factorial model fit from the NPSS engine deck data. Model generation was reiterated until R^2 and adjusted R^2 values are above 0.95 for the four models generated, which are: gross thrust, ram drag, fuel flow, and power split. These are modeled in terms of power code (PC), battery power input (Eboost), Mach number (MN) and altitude (alt). Higher than 2nd order full factorial model is not generated because the significance of higher order interactions are below 0.01 for each model.

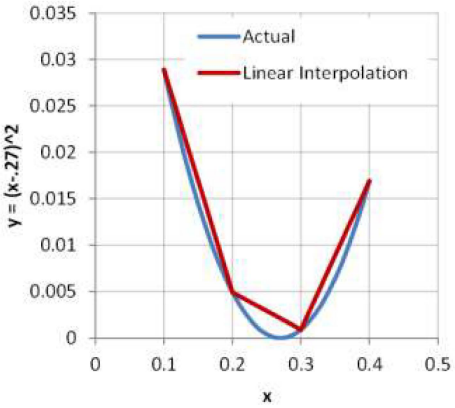

Fig. 6 Notional depiction of nonlinearity of an engine

Surrogate models are also utilized to reduce the computational strain. DDP is an algorithm that utilize linearized dynamics which assumes small disturbance. This means a single linearized dynamics model cannot be used for the whole mission or phase because the assumption is violated. So the dynamic has to be linearized at each timestep. The most fundamental way of differentiating a complex dynamic system is by performing finite differencing on the dynamics for each state and input with a small perturbation. Estimating a climb phase of 30 minutes and assuming that small disturbance assumption can be kept for 1 second then for each iteration a total of 1800 calculations are required. With a crude initial trajectory approximate number of iterations needed to converge the result to a local minimum is 1000 iterations. When finite differencing is performed on all the states and inputs during the each of the two forward propagation, total of 36 million engine deck query is needed per DDP iteration. This means the algorithm may not be fast enough to generate the flight trajectory on the fly. So a surrogate model is utilized to reduce the computational strain.

B. General Problem Statement

To properly simulate the flight of an aircraft, all of the aircraft state needs to be tracked including the aircraft weight and energy consumed. For a nonhybrid electric vehicle, weight calculation can be simplified as follows:

$$W_f = \min_{w_f} \int_{tstart}^{tend} w_f(t)dt \tag{23}$$

where w_f is fuel burn at given time step and W_f is the total fuel consumption, which is reiterated until it is converged to an initial assumed total fuel weight. The same method can be used to calculated the current weight of the aircraft for hybrid vehicle, but energy consumption also needs to be calculated to account for both battery and fuel states.

$$\dot{E} = P_{gas} + P_{electric} \tag{24a}$$

$$E_{electric} = E_{start} - \int_{t_0}^{t_f} e_{used} \tag{24b}$$

Both weight and energy states are added to the state vector so that DDP considers weight change of the aircraft during simulation and minimize energy consumption.

The objective function, J, utilized in this paper is the quadratic approximation of both state and input costs.

$$\Sigma_i^{N-1} J = \frac{1}{2}((x_i - x_f)^T Q(x_i - x_f) + u_i^T R u_i) + \frac{1}{2}(x_N - x_f)^T Q_f (x_N - x_f) \tag{25}$$

Where x is the state vector, Q is the running state weights , u is the input vector, R is the input weights, Q_f is the final state weights. There are many ways of modifying the results from this objective function. Firstly results are modified by changing the Q, Q_f, or by adding state constraints. Typically if the nominal optimal trajectory is unknow it is recommended to keep Q small and focus on Q_f. This way the algorithm is not in a rush at the earlier time steps to force the aircraft to reach the target. Impact of Q and Q_f on the result is discussed in the results section. Due to the scope of

this paper, state constraints are not implemented. This means the trajectory may violate certain flight path regulations. This issue can be addressed in the future through other variations of DDP such as constrained DDP[24].

Results are also modified by changing the R or by adding input constraints. A very large R would result in the aircraft failing to reach the target since focus is on minimizing the fuel use and not on reaching the target. Impact of R on the result is also discussed in the results section. Unlike, state constraint, input constraints are used to normalize and limit the inputs. This is necessary to refrain the DDP from using unrealistic inputs.

C. Aircraft Inputs

Based on the defined longitudinal dynamics, following parameters must be defined at every time step of the flight: drag, lift, thrust, energy consumed, and angle of attack. To define these parameters, following inputs are used:

$$\begin{pmatrix} PC \\ Eboost(MW) \\ n \\ \ddot{\theta}(rad/sec^2) \end{pmatrix} = \begin{pmatrix} PowerCode \\ ElectricPower \\ L/W \\ AngularAcceleration \end{pmatrix} \tag{26}$$

Drag is the accumulation of airframe drag, defined by Eq. 28 below, and ram drag of the engine. Gross thrust and ram drag are defined by PC, Eboost (MW), MN, and altitude (ft) at each time step. Eboost, fuel consumed (fallout of the engine deck), and specific energy of fuel (42MJ/kg) are integrated over the entire trajectory to obtained the energy consumed. Angle of attack is defined by integrating the angular acceleration over the entire trajectory. Angular acceleration is the input that represents the combined moment dynamics defined in Eq. 22c. Lift is defined with equation 27

$$nW = L = \frac{1}{2}\rho V^2 S C_L \tag{27}$$

where V (velocity) and ρ (density) are defined by the current state of the aircraft and S (wing area) is a fixed value. n, also known as L/W, is the input that determines the lift and C_L required at each time step to reach the desired trajectory. Airframe drag is obtained by the sum of induced and parasitic drag estimated using the drag polar calculated by FLOPS.

$$C_D = C_{D_0} + C_{D_i} \tag{28}$$

Parasitic drag, C_{D_0}, is defined by mach number and altitude of the current state, and induced drag, C_{D_i}, is defined by mach number and coefficient of lift.

All the inputs are limited with input constraint for two reasons. In the engine deck, the minimum and maximum values of power code and electric power are set. Also, in the dynamics, n and angular acceleration should be capped to match the realistic controls. Boundaries to each inputs are as follows

$$22 \leq PC \leq 50 \tag{29a}$$
$$0 \leq Eboost \leq 0.36 \tag{29b}$$
$$0.9 \leq n \leq 1.5 \tag{29c}$$
$$-0.001 \leq \ddot{\theta} \leq 0.001 \tag{29d}$$

where the PC and Eboost constraints are set by the engine deck data, n and $\ddot{\theta}$ are set by typical values of an aircraft. There are multiple ways of constraining the inputs including: clamping, squashing, and boxing methods [24]. Clamping method could diverge the algorithm by changing the direction of the optimization search path. Boxing method minimize the Q in terms of δu which requires modification in the DDP algorithm. Squashing function does introduce some none linearities but this can be assumed negligible if the time step is small enough. So squashing function is applied to each of the inputs. The squashing function is defined as follows

$$x_{i+1} = f(x_i, s(u_i)) \tag{30a}$$
$$\lim_{u \to -\infty} s(u) = \underline{b} \tag{30b}$$
$$\lim_{u \to \infty} s(u) = \bar{b} \tag{30c}$$

where s can any function such as a hyperbolic tangent or a sinusoid. The modified inputs are defined as follows

$$PC \rightarrow 14 * \tanh(PC - 4) + 36 \tag{31a}$$
$$Eboost \rightarrow .18105 * \tanh(Eboost) + .18105 \tag{31b}$$
$$n \rightarrow 0.275 * \tanh(n - 1.1513) + 1.225 \tag{31c}$$
$$\ddot{\theta} \rightarrow 0.001 * \tanh(\ddot{\theta}) \tag{31d}$$

Some benefits of using squashing constraint are the normalization of inputs and freedom to pick the input target. Normalization of input and state are important in defining the Q, Q_f, and R. For a given state and input cost weights, the significance of the weight vary based on the unit of the state or the input. Normalized state and input will clarify the relative significance of one state or input to another.

The reason why squashing constraint allows the user to modify the input target is shown in Fig.7. Note that the

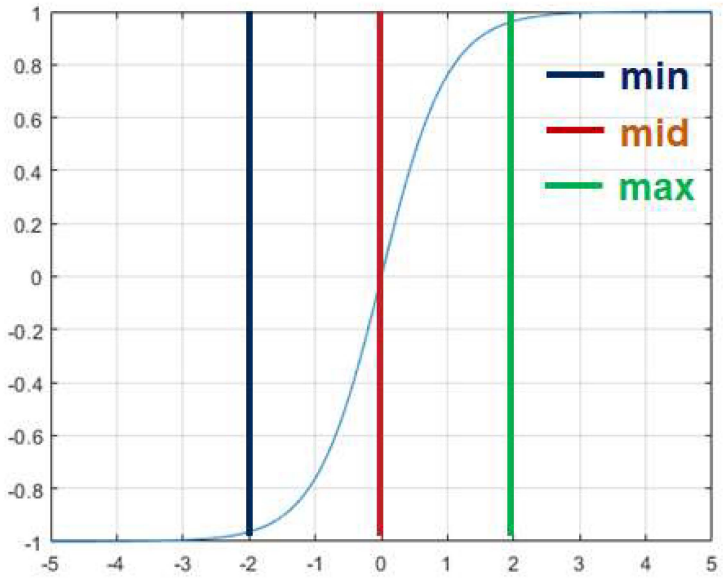

Fig. 7 Input targets set and min, mean, and max of the hyperbolic tangent function

objective function is a second order approximate of the true cost function. This means the DDP algorithm always try to find a input trajectory that would minimize the objective function. Also, modified in put replaces the corresponding input. This means if the hyperbolic tangent is shifted so that a modified input u_i would result in zero for the corresponding input, the DDP will try to converge at u_i instead of 0. The goal of PC, Eboost, n, and $\ddot{\theta}$ are 22, 0.36, 1, and 0 because this set of input minimizes the fuel burn and the structural stress on the aircraft. Hence PC and n inputs are shifted by -4 and -1.1513, respectively. Since the goal of this project is also to obtain the fuel burn minimizing power split trajectory, target Eboost trajectory is theoretically unknown. Hence, hyperbolic tangent of Eboost is not shifted to hit a specific target. The result of this behavior is discussed in the results section.

D. Initial Setup

Current method of determining coefficient of lift has the issue of getting an error at the beginning and the end of takeoff and landing (when velocity is 0). This issue compounds with the fact that ground roll of take off and landing cannot be represented by the dynamics of the aircraft without state constraints. To limit the scope of the paper, the

Table 2 Mission profile detail

Stage	Range (ft)	Altitude (ft)	MN	Time (min)
1: Start of Climb	0	0	0.25	0
2: Start of Cruise	.468E6	22.5E3	0.44	24
3: Start of Descent	3.178E6	22.5E3	0.44	123.5
4: Start of Approach	3.646E6	1.5E3	0.22	154

aircraft is set up to start the flight from the end of the takeoff phase.

$$\begin{pmatrix} x_0 \\ z_0 \\ \theta_0 \\ u_0 \\ w_0 \\ q_0 \\ E_0 \\ W_0 \end{pmatrix} = \begin{pmatrix} 0 \\ 0 \\ 0 \\ 300(ft/s) \\ 0 \\ 0 \\ 0 \\ 13123(lbm) \end{pmatrix} \tag{32}$$

The initial state trajectory is defined by the following initial input vector repeated for the first iteration

$$\begin{pmatrix} PC_0 \\ Eboost_0 \\ n_0 \\ \ddot{\theta} \end{pmatrix} = \begin{pmatrix} 8 \\ 0 \\ 0 \\ 0 \end{pmatrix} \tag{33}$$

E. Mission Profile

The analysis is performed on a section of climb phase determined by the flops output of a 9pax hybrid engine aircraft flown with a single climb, single cruise, and single approach flight phase as shown in Fig.8. For the current analysis,

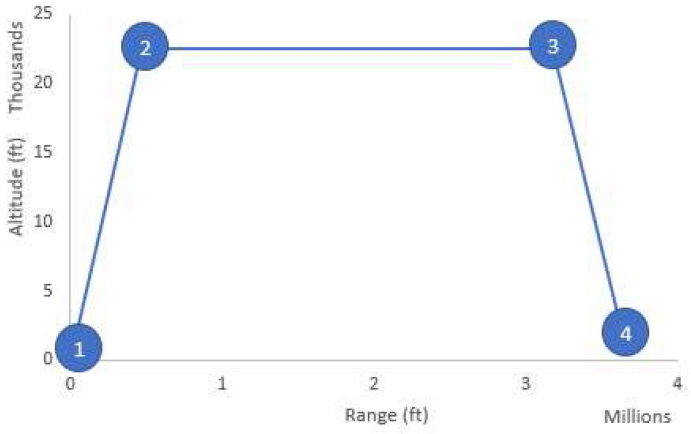

Fig. 8 Typical 9pax aircraft design mission

only the first segment of climb is analyzed due to two limitations:

1) Initial input trajectory for a full mission or any mission phase is unknown and optimization algorithm performance is unfavorable with poor initial point

2) The accumulated error for quadratic cost and linear dynamics increases with the horizon

Future work will consider the analysis from end of takeoff to beginning of landing ground roll with some modification on the algorithm. This is discussed in the final section of this paper.

The target trajectory at 170 seconds from takeoff is shown in equation 34

$$\begin{pmatrix} x_f \\ z_f \\ \theta_f \\ u_f \\ w_f \\ q_f \\ E_f \\ W_f \end{pmatrix} = \begin{pmatrix} 46852(ft) \\ 2250(ft) \\ 0 \\ 400(ft/s) \\ 0 \\ 0 \\ 0 \\ 13141.5(lbm) \end{pmatrix} \tag{34}$$

where x_f and z_f are one tenth of the entire climb phase, u_f is velocity value half way between start and end of climb, E_f is zero and W_f is same as initial weight since energy consumption needs to be minimized. The Q_f for each state parameters are set at 1000 except for weight Q_f is set at zero. Any value of Q_f for the weight state would double the significance of fuel consumed through energy and weight considerations. Q for each state parameters are set at 0 since the nominal trajectory is unknown. Finally R for each input parameters are set at 5000. This set up of the problem is be called the base setup.

VI. Results

A. Base Result With Varying Target Eboost

The state and input trajectory based on the above setup is shown in Fig.9 a fairly linear diagonal flight trajectory is

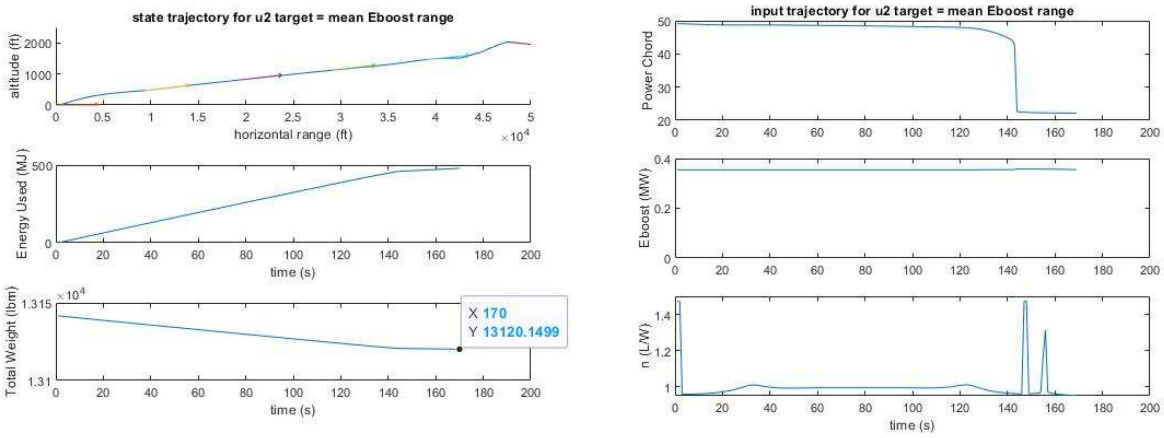

Fig. 9 State and input trajectory of the base setup

generated. The colored lies represent the angle of attack trajectory and it is approximately zero throughout the flight. Maximum PC and Eboost trajectories are used except for the last stretch where the PC is reduced to minimum but n is increased. This is because velocity state targets are met but position state targets are not. So the extra lift is used to reach the position targets. n is observed to peak once in beginning, twice near the end, and stay around 1 for the rest of the phase. The peaks for n trajectory are mainly because n is considered in the objective function. Whenever lift is generated, cost is applied to the objective function so the algorithm tries to minimize the time when lift is generated. So instantaneous lift is prefered, hence the peaks. These peaks are one of the reasons why the flight path angle of the final segments of the trajectory is slightly higher than the rest. Another reason is the fact that only final state cost is considered. Hence, the algorithm generated by this DDP is trying to minimize the cost throughout the flight but utilize

all the input to match the target state near the end of the mission. Effect of changing hyperparameters on the smoothness of the trajectory is observed later on. Overall the final weight of the aircraft is 13120.1 lbm which corresponds to 21.5lbm of fuel used.

The target value for Eboost has been modified to see if this would change the trajectory and overall consumption in Fig.10 and Fig.11. As the Fig.10 represents, maximizing the Eboost target does not change the result of the optimal

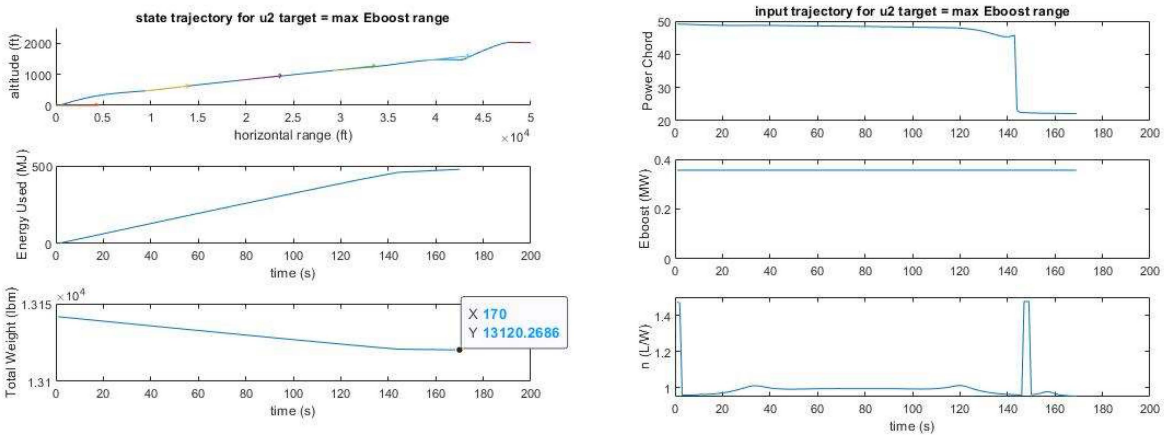

Fig. 10 State and input trajectory with Eboost target at 0.36MW

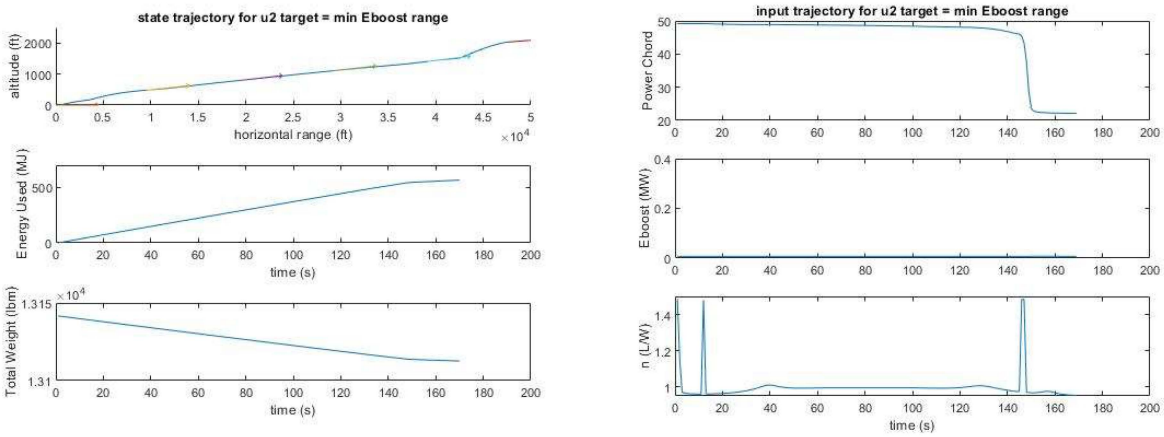

Fig. 11 State and input trajectory with Eboost target at 0MW

trajectory. This is because of the input and state cost contribution. Due to the number of parameters representing the aircraft state, the state cost has much bigger contribution to the objective function than the input cost. Hence, the input can be maximized but remain insignificant to the objective function. This is why setting the Eboost target at max and setting the Eboost target at the mean results in the same trajectory, as can be observed from Fig.9. However, minimizing the Eboost target results in a different trajectory where the electric power is unused for the entire climb phase. This is because, with the target Eboost at minimum, to use maximum Eboost, the input value has to increase by 16. Quadratic approximation of the objective function means this input will increase the input cost by 16^2, which does make input a significant component to minimize. The missing energy from the battery is satisfied by using more fuel, resulting in 7.5lbm higher fuel consumption for the second case.

B. Hybrid vs Conventional

One of the goal of this paper is to observe the impact that hybrid architecture has on the fuel consumption. To compare the fuel consumption of hybrid and non hybrid aircraft, two different non hybrid cases are generated. First is by

flying the same mission while forcing the Eboost to zero and reducing the aircraft weight by the battery weight, which is approximately 2070 lb for this engine. The result of this case is shown in Fig.12 A similar trajectory as the case where

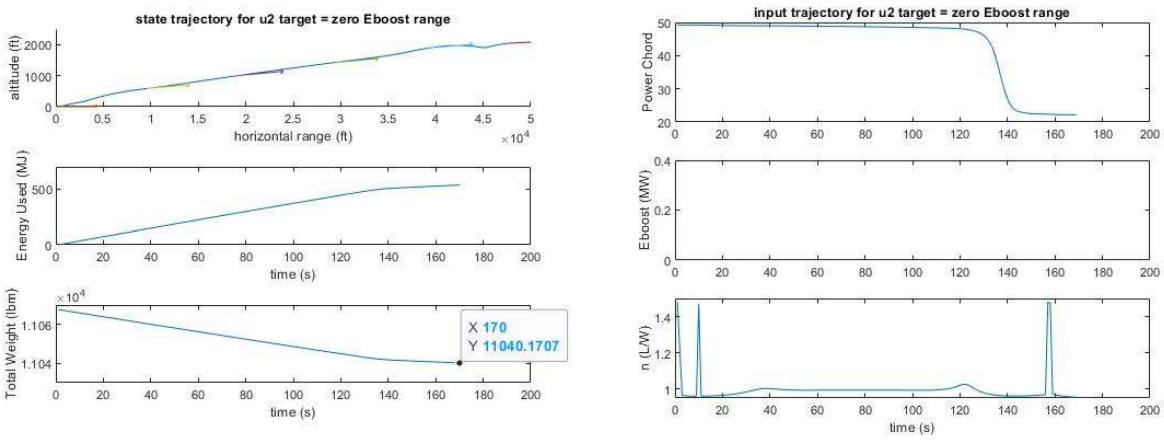

Fig. 12 State and input trajectory with Eboost forced to zero and reduced aircraft weight

Eboost is target at zero is observed with PC diminishing earlier for this case. This change is expected since weight of the aircraft decreased so there is no need to maintain full throttle. The final fuel consumption is 27.7 lbm, which is 6.2lbm higher than the base setup. This corresponds to energy consumption increasing from 478MJ to 536MJ for forced zero and base Eboost cases, respectively. If weight of the aircraft is reduced even further by removing the weight for all the electric components, fuel consumption is 1.3 lbm less for Eboost set to zero compared to base setup. This corresponds to reduction in energy consumption by 30MJ. These results validate the fact that weight is important factor when considering fuel burn reduction. So a modification in the code to obtain the flight and power split trajectories with limited electric and gas turbine energy source is necessary.

The second non hybrid case is generated by flying a 9 pax conventional turboprop aircraft same mission in FLOPS. The GTOW of the conventional aircraft is 12,475 lbm with design mission range of 700 nm, equivalent to the design mission range of the hybrid vehicle under study. DDP algorithm setup is modified to match the first half a segment of the FLOPS result with equation 35 and 36.

$$\begin{pmatrix} x_f \\ z_f \\ \theta_f \\ u_f \\ w_f \\ q_f \\ E_f \\ W_f \end{pmatrix} = \begin{pmatrix} 22785(ft) \\ 2310(ft) \\ 0 \\ 290(ft/s) \\ 0 \\ 0 \\ 0 \\ 13123(lbm) \end{pmatrix} \tag{35}$$

$$\begin{pmatrix} Q_f(x) \\ Q_f(z) \\ Q_f(\theta) \\ Q_f(u) \\ Q_f(w) \\ Q_f(q) \\ Q_f(E) \\ Q_f(W) \end{pmatrix} = \begin{pmatrix} 1000 \\ 10000 \\ 0 \\ 100 \\ 0 \\ 0 \\ 1000 \\ 0 \end{pmatrix} \tag{36}$$

The Q_f is modified so that altitude target is considered to be most significant. Since the goal of climb is to reach a desired altitude, the performace of hybrid aircraft result, generated with DDP, and conventional aircraft result, generated

with FLOPS, are compared at the altitude of 2310ft. angle of attack, change in angle of attack, vertical velocity and weight cost are set to zero since these states at the target are fallout of the climb phase trajectory. The DDP result with this setup is shown in Fig.13. Flight path trajectory observed is similar to the base configuration aircraft in Fig.9 with

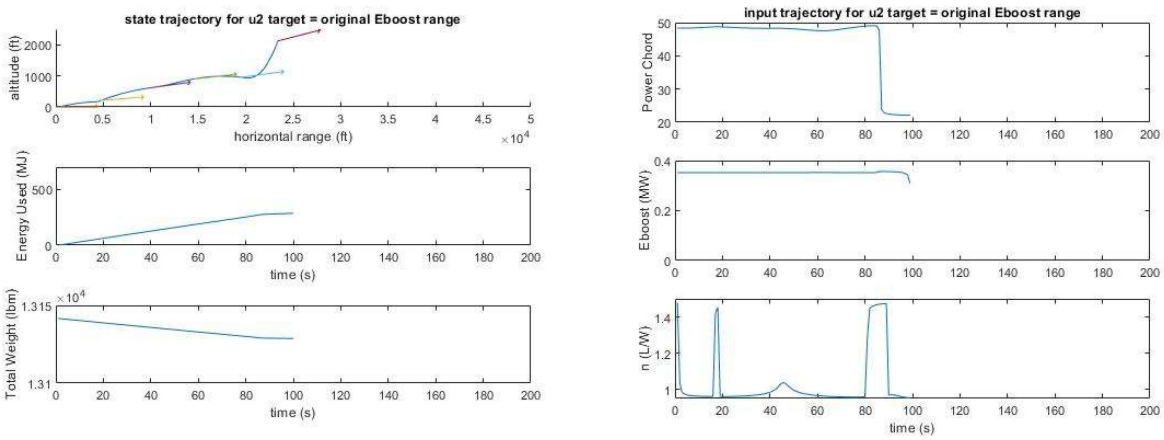

Fig. 13 State and input trajectory with modified target to match FLOPS result for 9pax aircraft

the exception of the last 5000 ft. A large increase in n is observed in the n input trajectory to meet the target. Larger lift is needed here than the base setup because the new setup is trying to reach the target at close to half the time. For the base setup 170 seconds are given while for the new setup only 80 seconds are given to match the FLOPS result. To address these abnormal behaviors, modification in the setup of the objective function, where the input cost is only defined by the energy parameters, is needed. Returning to the results, total fuel and energy consumed are 12.9 lbm and 287 MJ for the new setup. FLOPS result of the conventional aircraft's first segment of climb is shown in Table3 assuming that each parameter changes constantly with time, the final state of the FLOPS trajectory at altitude 2310 ft is

Table 3 FLOPS trajectory for the design mission

Time (min)	Alt (ft)	Range (ft)	Fuel (lbm)	Energy (MJ)
0	0	0	0	0
2.64	4620	45571	60.5	861
1.32	2310	22785	30.3	430

presented in the last row of Table3. The total fuel consumed for the conventional aircraft is 30.3 lbm which is 17.4 lbm higher than that of the hybrid aircraft. Based on the current results, hybrid architecture presents a sharp advantage over nonhybrid architecture. However, this result is based on a small segment of the mission. A significantly different result is expected when the algorithm is modified to analyze entire mission.

C. Impact of Varying State Hyperparameters On the State and Input Trajectory

Like any other optimization algorithm, DDP result is highly subceptable to how the hyperparemeters are setup. If a set of hyperparameters represents a single response surface of the objective function, then the response surface shifts and changes with a new set of hyperparameters. So it is critical to do trade study on the hyperparameters and optimize them.

Q_f, the final state cost, of all the states are increased by a magnitude of 10. This results in the diverging result where the algorithm bounced back and forth between two distinct trajectories. The direct reason for this is the relative magnitude of R and γ, the learning rate. R is not high enough or γ is not small enough to limit the δu calculated at each step. Underlying reason for this is that the algorithm is creating a 2nd order approximation of the objective function from the start of the "current" step. When δu is too large, the objective function approximation is no longer valid. Fig.14 is a good visualization of this phnomena. So R is increased by a magnitude of 20 and Fig.15 shows that the result is identical to that of the base setup. This is expected because as both state and input cost weights increase, their relative

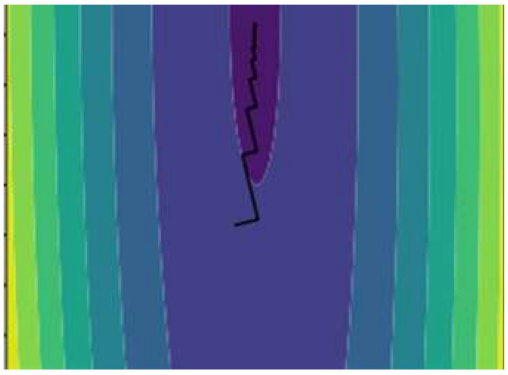

Fig. 14 Zigzag trajectory for searching the optimized point

contribution to objective function doesn't change. This shows that relative magnitude between state and input cost is of

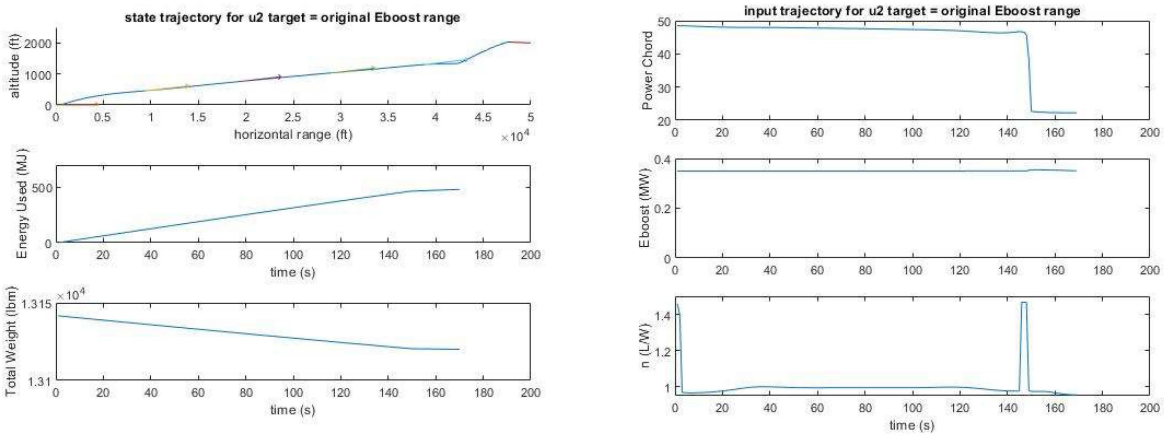

Fig. 15 State and input trajectory with Qf and R increased by magnitude of 10 and 20

importance.

Considering that some states may not be as important, result for increasing the final cost of velocity states by magnitude of 10 is observed in Fig.16. With the focus on the velocity states, the final steep climb to reach the target position is no longer observed. This is because the focus is now on matching the velocity vector and the flight path direction at the end of the trajectory. Based on the first plot in Fig.16, the algorithm exceeds the target altitude to match the velocity target while gliding down. This is because the target velocity is easier to match this way rather than using sharp maneuvers as the aircraft is climbing up, which would increase the input cost. A few bumps are observed along the flight path mainly due to the vertical velocity target. With the current setup, the priority is on matching the vertical velocity target of zero. Hence the aircraft is trying to fly horizontally as frequently as possible. To address this issue, it is necessary to consider time varying Q_f for future analysis.

Similar analysis is performed by only increasing the energy state final cost weight by a magnitude of 10, shown in Fig.17. The final trajectory obtained shows a significantly different behavior near the end of the flight path where a u shaped trajectory is observed. What increasing energy state final cost do to the algorithm is that the energy related inputs are minimized. Hence to minimize the input cost, power code is reduced at earlier time than usual, resulting in the drop. The loss of altitude from reduced power code is fixed by a significant increase in lift, a non energy input. In reality, increasing lift should is accompanied by increasing thrust to make up for the induced drag. This result again shows the need for separating the energy based and non energy based inputs from the objective function. Especially, if the focus of the problem is optimizing the use of two energy sources to generate enough thrust for a given mission. However, the trajectory is reasonable, mathmatically, since the aircraft was flying faster than the target velocity before the dip. So the extra drag is needed to meet the target velocity and minimize the objective function. Overall increasing

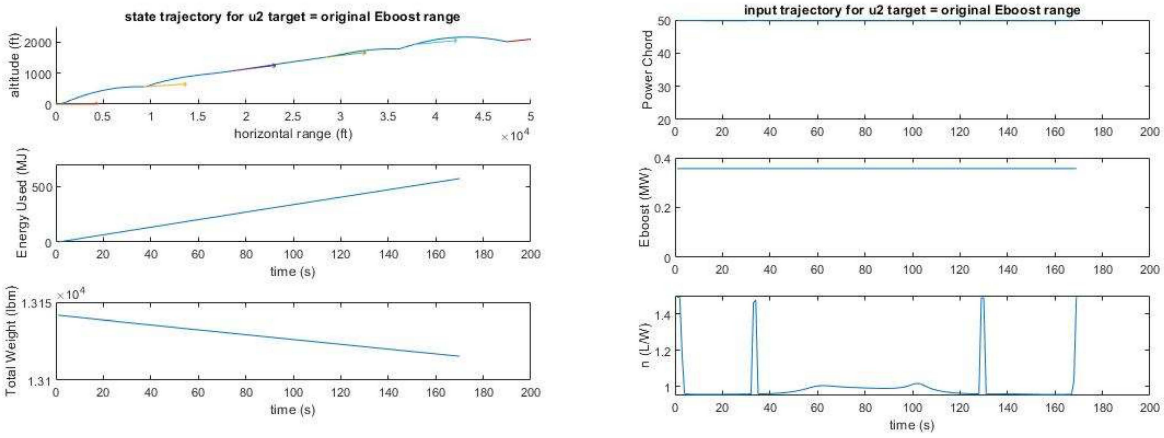

Fig. 16 State and input trajectory with Qf of velocity states increased by magnitude of 10

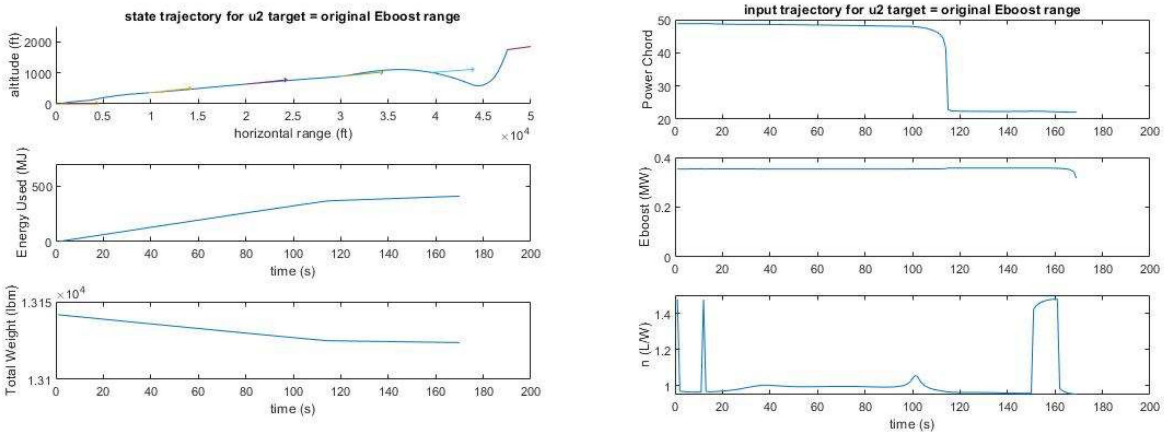

Fig. 17 State and input trajectory with Qf of energy state increased by magnitude of 10

the Q_f results in increasing the inputs to meet the desired target state.

This time Q_f for all the states are reduced and the results are shown in Fig.18 Reducing Q_f results in a very smooth 2 stage trajectory where a large flight path angle increase is observed near the end of the phase. Rest of the trajectories are similar to the base setup except the n trajectory becomes much smoother. A similar result is observed when only the energy state Q_f is reduced by magnitude of 10, as shown in Fig.19. As earlier results suggest, the extreme behaviors of input trajectories are mainly due to the constraint on the input. PC is reduced near the end of the trajectory to minimize the objective function. This is not the case when the energy state Q_f is reduced. With this case, PC maintained maximum trajectory, as it should for typical aircraft climb. Hence, the additional lift is no longer required to meet the target, so the peaks in n are no longer observed. Overall this results in a very smooth trajectory with no sudden changes in the flight path angle. This again speaks for the importance of hyperparameter optimization, because even for a energy minimizing problem, the cost weight on energy cannot be too high to obtain a smooth, preferable trajectory. The downfall of this prefereable trajectory is that fuel consumption, which is increased by 5lbm from the base setup. The smoothness of the trajectory and the amount energy saved should be accessed depending on the situation.

D. Impact of Varying Input Hyperparameters On the State and Input Trajectory

Input cost is modified to observe the the impact of R on the trajectory. Just like when the all the state final costs were increased by 10, reducing input cost by 10 results in a diverging solution. The same reason applies to the divergence. The trajectory for increasing R is shown in Fig.20. First thing to point out is that the trajectory did not meet the target

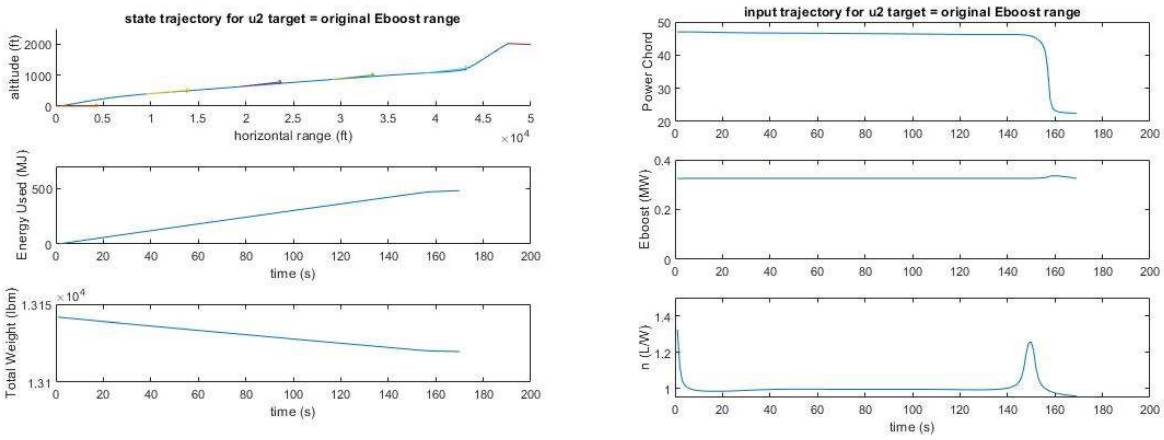

Fig. 18 State and input trajectory of all states Qf reduced by magnitude of 10

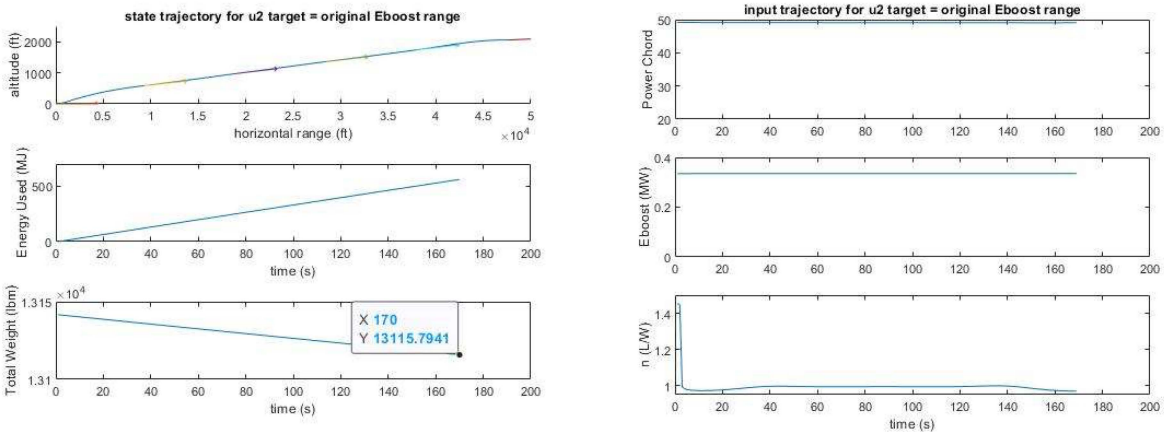

Fig. 19 State and input trajectory of all states Qf reduced by magnitude of 10

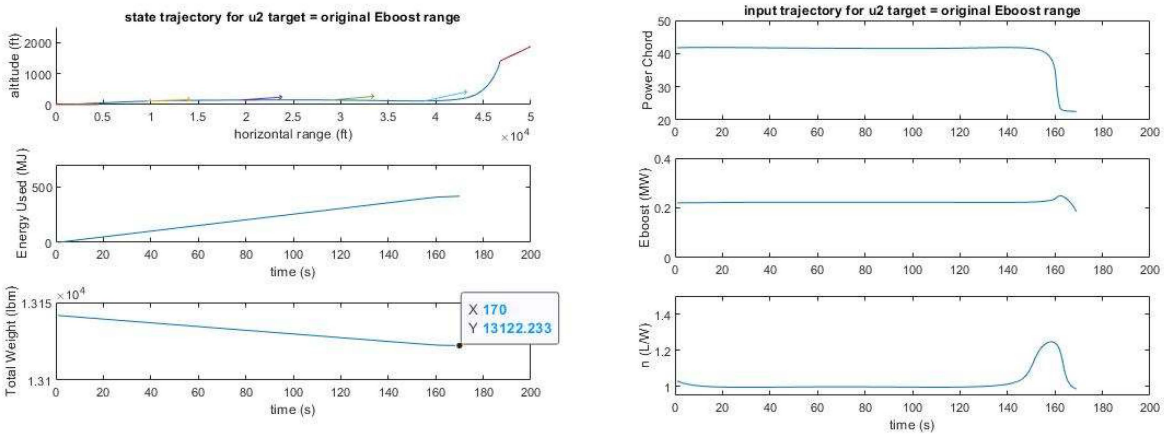

Fig. 20 State and input trajectory of R increased by magnitude of 10

at the end of 1000th iteration. This implies that when the input cost is too high, there is not enough input to create a trajectory to meet the target. The trajectory obtained with this setup tries to fly near the surface and then shoots up near

the end to reach the target. Notice, a big contributor to this behavior is the extra constraint on n. Again the need to separate the energy and non energy inputs for the objective function setup.

VII. Conclusion and Future Work

boring Eboost Current aerospace industry has a need to reduce emission and generate optimized trajectories on the fly to assist pilots. Hybrid architecture has a potential to meet the target emission. However, hybrid architecture comes with a need to find the optimal power split trajectory. A method, that utilize differential dynamic programming, is introduced to simultaneously optimize the power management and the trajectory to satisfy both goals. The fuel and energy consumption for hybrid and non hybrid architectures of 9pax aircraft is compared to demonstrate the potential of the method introduced. It is found that for a segment of climb, fuel burn reducing trajectory can be generated with the proposed methodology. Furthermore, the hybrid architecture aircraft resulted in 6.5lbm of reduced fuel burn than conventional architecture aircraft assuming that battery power can be maximized at 0.36MW for the entire flight segment. The most fuel efficient trajectory for PC is maximized PC for majority of the climb but reducing PC near the end of trajectory. Finishing the climb with increasing lift by modifying the airframe configuration instead of engine thrust. As expected, the most fuel efficient trajectory for Eboost is maximized Eboosts for the entire climb.

Its important to realize that the current result is limited to a small segment of the entire mission. Also, fuel and battery capacities are not considered during the analysis. The trivial trajectories are prone to change when more phases of the mission are included in the future. However, it is shown that simultaneous optimization of flight and power split trajectory can be done with the proposed methodology. Finally, the potential for this methodology to be used for a general mission is shown by performing the conventional architecture aircraft mission on the hybrid architecture aircraft.

Some observations based on the trade studies are listed below with the future work to potentially improve the results, especially to better assist the pilots on flight trajectory generation.

1) Utilize time variant hyperparameters to better simulate the flight condition
2) Modify the objective function to only consider energy based inputs
3) Use a better initial trajectory to generate full mission trajectory
4) Apply constraint DDP to add physical and legal flight constraints

These future works are necessary to improve the trajectories generated through the proposed methodology. Interesting future investigations to expand the scope of the methodology are listed below.

1) Use nonlinear DDP variant to reduce computation time and accuracy of the model
2) Apply min max DDP variant algorithm and set the two energy source to compete to minimize fuel consumption
3) Aircraft sizing by reiterating the algorithm until total fuel and battery weight are converged to the initial assumed weights
4) Modify the target states per time step and utilize receeding horizon to run the full mission on the fly
5) Perform hyperparameter optmization to further optimize the trajectory and reduce fuel consumption

References

[1] "The World of Air Transport in 2018," , 2019. URL https://www.icao.int/annual-report-2018/Pages/the-world-of-air-transport-in-2018.aspx.

[2] Jansen, R., Bowman, C., Jankovsky, A., Dyson, R., and Felder, J., "Overview of NASA Electrified Aircraft Propulsion (EAP) Research for Large Subsonic Transports," *53rd SAE/ASEE Jt. Propuls. Conf*, 2017, p. 1– 20.

[3] Rutherford, D., "Size matters for aircraft fuel efficiency. Just not in the way that you think." , Feb. 2018. URL https://theicct.org/blog/staff/size-matters-for-aircraft-fuel-efficiency.

[4] Balin, M., "ARMD Strategic Thrust 6: Assured Autonomy for Aviation Transformation," Tech. rep., NASA AERONAUTICS, May 2016.

[5] Sun, W., Pan, Y., Lim, J., Theodorou, E., and Tsiotras, P., "Min-Max Differential Dynamic Programming: Continuous and Discrete Time Formulations," *Journal of Guidance, Control, and Dynamics*, Vol. 41, 2018, pp. 1–13. doi:10.2514/1.G003516.

[6] Xie, Z., Liu, C., and Hauser, K., "Differential dynamic programming with nonlinear constraints," 2017, pp. 695–702. doi:10.1109/ICRA.2017.7989086.

[7] Heppeler, G., Sonntag, M., and Sawodny, O., "Fuel efficiency analysis for simultaneous optimization of the velocity trajectory and the energy management in hybrid electric vehicles," *IFAC Proceedings Volumes (IFAC-PapersOnline)*, Vol. 19, 2014, pp. 6612–6617.

[8] Mavris, D., Nam, T., and Cinar, G., "Alternate Energy Based Sizing Method," , 2019. Fall 2019 AE 6343 Lecture for Georgia Institute of Technology.

[9] Becerra, V., "Optimal Control," Vol. 3, No. 1, 2008. doi:10.4249/scholarpedia.5354, revision 124632.

[10] Milios, K., "Power Management of Hybrid-Electric Aircraft Using NPSS," , 2018.

[11] Trawick, D., Milios, K., Gladin, J., and Mavris, D. N., "A Method for Determining Optimal Power Management Schedules for Hybrid Electric Airplanes," *Propulsion and Energy 2019 Forum*, 2019. Doi: 10.2514/6.2019-4500.

[12] Nino-Baron, C., Rehman, A., Zhu, G., and Strangas, E., "Trajectory Optimization for the Engine–Generator Operation of a Series Hybrid Electric Vehicle," *Vehicular Technology, IEEE Transactions on*, Vol. 60, 2011, pp. 2438 – 2447. doi:10.1109/TVT.2011.2141695.

[13] Falck, R. D., Chin, J., Schnulo, S. L., Burt, J. M., and Gray, J. S., "Trajectory Optimization of Electric Aircraft Subject to Subsystem Thermal Constraints," *18th ISSMO Multidisciplinary Analysis and Optimization Conference*, 2017. Doi: 10.2514/6.2017-4002.

[14] Cinar, G., "A Methodology For Dynamic Sizing of Electric Power Generation and Distribution Architectures," Ph.D. thesis, Georgia Institute of Technology, Daniel Guggenheim School of Aerospace Engineering, Atlanta, GA, 2018.

[15] Sun, W., Theodorou, E., and Tsiotras, P., "Continuous-time differential dynamic programming with terminal constraints," 2014, pp. 1–6. doi:10.1109/ADPRL.2014.7010647.

[16] of Computer Science Center for Intelligent Machines, M. S., "Trajectory Optimization," , Oct. 2017. Lecture COMP 765.

[17] Liao, L. ., and Shoemaker, C. A., "Convergence in unconstrained discrete-time differential dynamic programming," *IEEE Transactions on Automatic Control*, Vol. 36, No. 6, 1991, pp. 692–706.

[18] Todorov, E., and Li, W., "Optimal control methods suitable for biomechanical systems," 2003, pp. 1758 – 1761 Vol.2. doi:10.1109/IEMBS.2003.1279748.

[19] Morimoto, J., Zeglin, G., and Atkeson, C., "Minimax differential dynamic programming: application to a biped walking robot," 2003, pp. 1927 – 1932 vol.2. doi:10.1109/IROS.2003.1248926.

[20] Pellegrini, E., "Multiple-Shooting Differential Dynamic Programming with Applications to Spacecraft Trajectory Optimization," Ph.D. thesis, The University of Texas at Austin, Austin, TX, 06 2017.

[21] Grebe, N., "Differential Dynamic Programming for Aerial Robots using an Aerodynamics Model," 2017.

[22] Caughey, D., "Introduction to Aircraft Stability and Control," , 2011. M and AE 5070 lecture for Cornell University.

[23] Etkin, B., *Dynamics of flight : stability and control*, 3rd ed., Wiley, New York, 1995.

[24] Tassa, Y., Mansard, N., and Todorov, E., "Control-limited differential dynamic programming," 2014. doi:10.1109/ICRA.2014.6907001.